Kshma Trivedi, Santanu Koley

MOTIONS OF A FREELY FLOATING THICK RIGID STRUCTURE OVER ASYMMETRIC TRENCHES

KRETANJE SLOBODNO PLUTAJUĆE DEBELOZIDE KRUTE KONSTRUKCIJE NAD ASIMETRIČNIM ROVOVIMA

Originalni naučni rad / Original scientific paper
UDK /UDC:

Rad primljen / Paper received: 6.4.2021

Adresa autora / Author's address:
Department of Mathematics, Birla Institute of Technology and Science-Pilani, Hyderabad Campus, India
email: p20190439@hyderabad.bits-pilani.ac.in , santanu@hyderabad.bits-pilani.ac.in

Keywords
- radiation
- boundary element method (BEM)
- heave
- surge
- pitch

Ključne reči
- prostiranje talasa
- metoda graničnih elemenata (MGE)
- odizanje
- udar
- naginjanje

Abstract

The present study analyses the motions of freely floating rigid structures over the asymmetric trenches. The boundary value problem (BVP) is solved using the boundary element method (BEM). Various physical parameters such as radiation damping and added mass associated with the surge, heave and pitch motions of the freely floating body over the asymmetric trenches are studied for various values of dock length. The study shows that the damping coefficient and added mass correspond to the heave and pitch motions of the rigid dock increases with an increase in dock length. In addition, the added mass and damping coefficient related to the surge motion of the floating dock increases with an increase in dock length in the long wave regime. Nevertheless, reverse pattern is noticed in the intermediate wave regime. Moreover, there is no significant effect of dock length on the damping coefficient and added mass that correspond to surge motion in the short-wave regime.

Izvod

U radu je prikazana analiza kretanja slobodno plutajuće krute konstrukcije nad asimetričnim rovovima. Granični zadatak se rešava metodom graničnih elemenata (MGE). Razmotreni su izvesni fizički parametri radi određivanja vrednosti dužine doka, na primer, prigušenje talasa i dodatak mase povezano sa kretanjem slobodno plutajućeg tela nad asimetričnim rovovima, tipa udar, odizanje i naginjanje. Istraživanje pokazuje da koeficijent prigušenja i dodata masa, koji odgovaraju kretanjima tipa odizanje i naginjanje krutog doka se povećavaju sa povećanjem dužine doka. Pored toga, dodata masa i koeficijent prigušenja povezani sa udarnim kretanjem plutajućeg doka rastu sa porastom dužine doka u dugotalasnom režimu. Međutim, uočava se obrnuti šablon kod srednjetalasnog režima. Štaviše, dužina doka nema značajnog uticaja na koeficijent prigušenja i dodatu masu koji odgovaraju udarnom kretanju u kratkotalasnom režimu.

INTRODUCTION

The motion of freely floating body in various modes (degrees of freedom) has a large number of applications in ocean engineering and naval architecture fields. These free motions are used to analyse the hydrodynamics around a ship or floating offshore breakwater/wave barrier. This particular field of study is often referred as water waves radiation problem. In the literature, most of the research works are done by considering the rigid body floating over uniform water bed. However, since the ocean bed is non-uniform in nature and often the bottom topography consists of trenches, the analysis of freely floating rigid bodies over undulated bottom topography is utmost important. Lee /1/ used analytical method to analyse the radiation problem corresponding to the heave motion of a floating structure and it is concluded that the water depth is linearly proportional to the added mass and inversely proportional to the coefficient associated with damping. Hsu and Wu /2/ studied the radiation problem by the floating rectangular structure placed near a vertical rigid sea wall. It is reported that the radiation damping and added mass depend on the structural configurations such as submergence depth, width of the structure and gap between the structure and the sidewall. Williams et al. /3/ used the BEM to investigate the performance of dual pontoon type floating breakwaters of rectangular cross-section and it is shown that the radiation damping coefficients approach zero in short wave and long-wave regimes. Zheng et al. /4/ used analytical method to study the diffraction and radiation of water waves by floating buoy and calculated various physical quantities such as the radiation damping, added mass and the wave excitation forces associated with the motions of the floating rectangular buoy. Zheng et al. /5/ studied the diffraction and radiation problems of water waves by rectangular shape floating body situated near the sea wall. It is concluded that the added mass increases, wave force and radiation damping decrease with an increase in structural width. Shen et al. /6/ analysed the hydrodynamic effect of bottom sill on the radiation damping, added mass and wave excitation forces. In this study, the following conclusions are obtained: (i) the added mass in heave motion is directly proportional to the sill height ratio, whilst the variation of sill height has negligible effects on the damping coefficient; (ii) in intermediate and shallow water regions, the sill height ratio significantly increases the reflection coefficients, and reverse pattern is noticed for the transmission coefficient. Zheng et al. /7/ studied the radiation problem of a floating body in oblique incoming waves. It is reported that (i) the wave excitation force decreases with an increase in structural width, and (ii) the damping coefficients and added mass are directly proportional to the structural width. Zhou et al. /8/ studied the diffraction and radiation problems of a floating rectangular body with an opening in its lower side. It is observed that the resonance occurs due to the piston mode, and the sloshing phenomena have pivotal effect on the excitation forces and vertical motion. Zheng and Zhang /9/ investigated the diffraction and radiation of water waves by multiple rectangular floaters. It is reported that the structural width significantly affects the transmission coefficient.

In this paper, the surge, heave and pitch motions of the thick rigid dock floating over asymmetric bottom trenches are studied using the BEM. The bottom trench consists of two asymmetric trenches situated in series.

MATHEMATICAL FORMULATION AND SOLUTION METHODOLOGY

This section provides the mathematical modelling of freely floating thick rigid structure over the asymmetric trenches. For the mathematical modelling, the 2D Cartesian coordinate system is considered as shown in Fig. 1. A thick floating rigid structure having width $2a$ occupies the region $-a < x < a$ along the x-axis and the body freely oscillates at the free surface $z = 0$. Further, the submergence depth of the rigid body in the water is d. The thick floating structure is placed over the asymmetric rectangular trenches of width w_1 and w_2, in respect. The two asymmetric trenches occupy the region $-b_1 < x < -b_2$, $-h_2 < z < 0$ and $c_1 < x < c_2$, $-h_4 < z < 0$, respectively. In the present study, the solution methodology is based on BEM. In BEM, the physical domain should be closed. Therefore, two auxiliary boundaries Γ_{c1} and Γ_{c2} are considered at $x = -l$ and $x = r$, respectively. The total bottom and mean free surface boundaries are denoted by Γ_b and Γ_f, respectively. Further, $\Gamma_{d1} = \{x = -a,\ -d < z < 0\}$, $\Gamma_{d2} = \{-a < x < a,\ z = -d\}$, and $\Gamma_{d3} = \{x = a,\ -d < z < 0\}$ represent the submerged boundaries of the floating rigid dock. Moreover, the water flow is taken as potential kind, and the motion is simple harmonic in time. The velocity potential associated with the radiated waves is expressed as $\psi^R(x,z,t) = \Re\{-i\sigma A^{R,L}\psi^{R,L}(x,z)e^{-i\sigma t}\}$, where: $A^{R,L}$ represent the amplitude of the motion of the rigid dock with $L = 1,2,3$ indicate the heave, surge, and pitch motions, respectively. For the pitch motion, the centre of rotation is considered as (0,0). With these assumptions, the governing equation is given by

$$\frac{\partial^2\psi^{R,L}}{\partial x^2}+\frac{\partial^2\psi^{R,L}}{\partial z^2}=0\,. \quad (1)$$

The boundary condition (bc) on the free surface Γ_f yields

$$\frac{\partial\psi^{R,L}}{\partial n}-K\psi^{R,L}=0,\quad \text{on}\ \Gamma_f\,, \quad (2)$$

where: $\partial/\partial n$ represents the derivative in the normal direction on the corresponding boundaries. The bc on Γ_b is given by

$$\frac{\partial\psi^{R,L}}{\partial n}=0,\quad \text{on}\ \Gamma_b\,. \quad (3)$$

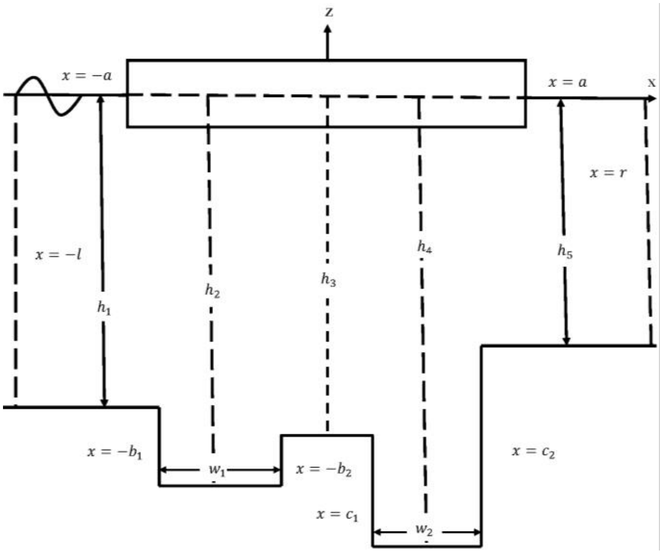

Figure 1. Schematic of the physical problem.

The rigid dock bcs on $\Gamma_{d1}\cup\Gamma_{d2}\cup\Gamma_{d3}$ are given by (see Zheng et al. /4/ for details),

$$\frac{\partial\psi^{R,1}}{\partial n}=\delta_{2j},\quad \text{on}\ \Gamma_{dj},\ \ j=1,2,3\,, \quad (4)$$

$$\frac{\partial\psi^{R,2}}{\partial n}=\delta_{1j}-\delta_{3j},\quad \text{on}\ \Gamma_{dj},\ \ j=1,2,3\,, \quad (5)$$

$$\frac{\partial\psi^{R,3}}{\partial n}=z(\delta_{1j}-\delta_{3j})-x\delta_{2j},\quad \text{on}\ \Gamma_{dj},\ \ j=1,2,3\,. \quad (6)$$

Finally, the far-field bcs are given by

$$\begin{cases}\dfrac{\partial\psi^{R,L}}{\partial n}-ik_0\psi^{R,L}=0, & \text{on}\ \Gamma_{c1}\\[2mm] \dfrac{\partial\psi^{R,L}}{\partial n}-ip_0\psi^{R,L}=0, & \text{on}\ \Gamma_{c2}\end{cases} \quad (7)$$

Here, k_0 and p_0 are positive real roots of the dispersion relations $\omega^2 = gk\tanh kh_1$ and $\omega^2 = gp\tanh ph_5$, respectively.

To solve the above BVP problem, the BEM technique is used. In this solution methodology, firstly, we transform the radiated velocity potential $\psi^{R,L}$ for $L = 1,2,3$ into a system of Fredholm integral equations. These are transformed into the system of equations using the BEM. Now, the Green's function $G(x,z;p,q)$ is represented by

$$G(x,z;p,q)=\frac{-\ln(\hat r)}{2\pi},\quad \hat r=\sqrt{(x-p)^2+(z-q)^2}\,. \quad (8)$$

Now, applying Green’s theorem on $\psi^{R,L}$ and $G(x,z;p,q)$ and using boundary conditions Eqs.(2)-(7), the following integral equations for $\psi^{R,L}$ ($L = 1,2,3$) are obtained as (see Katsikadelis /10/ for details).

$$C\psi^{R,1}+\int_{\Gamma_f}\left(\frac{\partial G}{\partial n}-KG\right)\psi^{R,1}d\Gamma+\int_{\Gamma_{c1}}\left(\frac{\partial G}{\partial n}-ik_0G\right)\psi^{R,1}d\Gamma+\int_{\Gamma_{d1}}\psi^{R,1}\frac{\partial G}{\partial n}d\Gamma+\int_{\Gamma_{d2}}\psi^{R,1}\frac{\partial G}{\partial n}d\Gamma+\int_{\Gamma_{d3}}\psi^{R,1}\frac{\partial G}{\partial n}d\Gamma+\int_{\Gamma_b}\psi^{R,1}\frac{\partial G}{\partial n}d\Gamma+$$
$$+\int_{\Gamma_{c2}}\left(\frac{\partial G}{\partial n}-ip_0G\right)\psi^{R,1}d\Gamma=\int_{\Gamma_{d2}}Gd\Gamma, \tag{9}$$

$$C\psi^{R,2}+\int_{\Gamma_f}\left(\frac{\partial G}{\partial n}-KG\right)\psi^{R,2}d\Gamma+\int_{\Gamma_{c1}}\left(\frac{\partial G}{\partial n}-ik_0G\right)\psi^{R,2}d\Gamma+\int_{\Gamma_{d1}}\psi^{R,2}\frac{\partial G}{\partial n}d\Gamma+\int_{\Gamma_{d2}}\psi^{R,2}\frac{\partial G}{\partial n}d\Gamma+\int_{\Gamma_{d3}}\psi^{R,2}\frac{\partial G}{\partial n}d\Gamma+\int_{\Gamma_b}\psi^{R,2}\frac{\partial G}{\partial n}d\Gamma+$$
$$+\int_{\Gamma_{c2}}\left(\frac{\partial G}{\partial n}-ip_0G\right)\psi^{R,2}d\Gamma=\int_{\Gamma_{d1}}Gd\Gamma-\int_{\Gamma_{d3}}Gd\Gamma, \tag{10}$$

$$C\psi^{R,3}+\int_{\Gamma_f}\left(\frac{\partial G}{\partial n}-KG\right)\psi^{R,3}d\Gamma+\int_{\Gamma_{c1}}\left(\frac{\partial G}{\partial n}-ik_0G\right)\psi^{R,3}d\Gamma+\int_{\Gamma_{d1}}\psi^{R,3}\frac{\partial G}{\partial n}d\Gamma+\int_{\Gamma_{d2}}\psi^{R,3}\frac{\partial G}{\partial n}d\Gamma+\int_{\Gamma_{d3}}\psi^{R,3}\frac{\partial G}{\partial n}d\Gamma+\int_{\Gamma_b}\psi^{R,3}\frac{\partial G}{\partial n}d\Gamma+$$
$$+\int_{\Gamma_{c2}}\left(\frac{\partial G}{\partial n}-ip_0G\right)\psi^{R,3}d\Gamma=\int_{\Gamma_{d1}}zGd\Gamma-\int_{\Gamma_{d2}}xGd\Gamma-\int_{\Gamma_{d3}}zGd\Gamma. \tag{11}$$

Now, using constant elements and point collocation method, Eqs.(9)-(11) are transformed into a system of linear algebraic equations as follows (see Koley and Trivedi /11/ for detailed derivations),

$$\left([H]-K[G]\right)\left[\psi^{R,1}\right]|_{\Gamma_f}+\left([H]-ik_0[G]\right)\left[\psi^{R,1}\right]|_{\Gamma_{c1}}+[H]\left[\psi^{R,1}\right]|_{\Gamma_{d1}}+[H]\left[\psi^{R,1}\right]|_{\Gamma_{d2}}+[H]\left[\psi^{R,1}\right]|_{\Gamma_{d3}}+[H]\left[\psi^{R,1}\right]|_{\Gamma_b}+$$
$$+\left([H]-ip_0[G]\right)\left[\psi^{R,1}\right]|_{\Gamma_{c2}}=[G]|_{\Gamma_{d2}}, \tag{12}$$

$$\left([H]-K[G]\right)\left[\psi^{R,2}\right]|_{\Gamma_f}+\left([H]-ik_0[G]\right)\left[\psi^{R,2}\right]|_{\Gamma_{c1}}+[H]\left[\psi^{R,2}\right]|_{\Gamma_{d1}}+[H]\left[\psi^{R,2}\right]|_{\Gamma_{d2}}+[H]\left[\psi^{R,2}\right]|_{\Gamma_{d3}}+[H]\left[\psi^{R,2}\right]|_{\Gamma_b}+$$
$$+\left([H]-ip_0[G]\right)\left[\psi^{R,2}\right]|_{\Gamma_{c2}}=[G]|_{\Gamma_{d1}}-[G]|_{\Gamma_{d3}}, \tag{13}$$

$$\left([H]-K[G]\right)\left[\psi^{R,3}\right]|_{\Gamma_f}+\left([H]-ik_0[G]\right)\left[\psi^{R,3}\right]|_{\Gamma_{c1}}+[H]\left[\psi^{R,3}\right]|_{\Gamma_{d1}}+[H]\left[\psi^{R,3}\right]|_{\Gamma_{d2}}+[H]\left[\psi^{R,3}\right]|_{\Gamma_{d3}}+[H]\left[\psi^{R,3}\right]|_{\Gamma_b}+$$
$$+\left([H]-ip_0[G]\right)\left[\psi^{R,2}\right]|_{\Gamma_{c2}}=[z][G]|_{\Gamma_{d1}}-[x][G]|_{\Gamma_{d2}}-[z][G]|_{\Gamma_{d3}}. \tag{14}$$

Finally, the discrete values of $\psi^{R,L}$ and $\partial\psi^{R,L}/\partial n$ are obtained over each boundary element of the total boundary.

RESULTS AND DISCUSSION

In this section, various results corresponding to the radiation problem by a floating rigid dock over asymmetric trenches are analysed. The geometrical and incident wave parameters are taken as: $h_1 = 10$ m; $h_2 = 2h_1$; $h_3 = 1.5h_1$; $h_4 = 3h_1$; $h_5 = 0.5h_1$; $d = 0.2h_1$; $b_1 = h_1$; $b_2 = 0.5h_1$; $c_1 = 0.5h_1$; $c_2 = h_1$ and $g = 9.81$ m/s^2. The expressions for the added mass (AM) and radiation damping (RD) are given by

$$\tilde{m}_{L,j}=\rho\int_{\Gamma_{d1}\cup\Gamma_{d2}\cup\Gamma_{d3}}\Re\left[\psi^{R,L}\right]n_j d\Gamma,\quad \text{for } L=1,2,3, \tag{15}$$

$$\tilde{N}_{L,j}=\rho\sigma\int_{\Gamma_{d1}\cup\Gamma_{d2}\cup\Gamma_{d3}}\Re\left[\psi^{R,L}\right]n_j d\Gamma,\quad \text{for } L=1,2,3, \tag{16}$$

where: $n_1 = \cos(n,z)$, $n_2 = \cos(n,x)$, and $n_3 = zn_2 - xn_1$. Therefore, the non-dimensional form of AM and RD are given by

$$m_{1,1}=\tilde{m}_{1,1}/2\rho h_1^2,\quad N_{1,1}=\tilde{N}_{1,1}/2\sigma\rho h_1^2, \tag{17}$$

$$m_{2,2}=\tilde{m}_{2,2}/2\rho h_1^2,\quad N_{2,2}=\tilde{N}_{2,2}/2\sigma\rho h_1^2, \tag{18}$$

$$m_{3,3}=\tilde{m}_{3,3}/2\rho h_1^3,\quad N_{3,3}=\tilde{N}_{3,3}/2\sigma\rho h_1^3. \tag{19}$$

Figures 2a and 2b depict the variation of AM $m_{1,1}$ and RD coefficient $N_{1,1}$ correspond to the heave motion of the floating dock as a function of wavenumber $\hat{K}$ for various values of dock length $\hat{a}$. Figure 2a illustrates that $m_{1,1}$ increases as $\hat{K}$ becomes higher. Further, it is noted that the $m_{1,1}$ increases as $\hat{a}$ increases. In Figure 2b, it is observed that the $N_{1,1}$ decreases as $\hat{K}$ increases. Moreover, for long waves, the $N_{1,1}$ increases as $\hat{a}$ increases, and the variation in the $N_{1,1}$ due to the dock length is negligible in the short-wave regime.

Figures 3a and 3b illustrate the variation of AM $m_{2,2}$ and RD $N_{2,2}$ correspond to the surge motion of the floating dock as a function of dimensionless wavenumber $\hat{K}$ for various values of dock length $\hat{a}$. In Fig. 3a, it is observed that $m_{2,2}$ decreases as $\hat{K}$ increases. Further, for short-waves, variation in the $m_{2,2}$ is negligible for various dock length $\hat{a}$. Figure 3b depicts that the $N_{2,2}$ initially increases with an increase in $\hat{K}$ and attains maximum. Hereafter, in the intermediate and shortwave regime, $N_{2,2}$ decreases as $\hat{K}$ increase. Moreover, for long waves, the $N_{2,2}$ increases with an increase in $\hat{a}$, and this variation is negligible in the shortwave regime.

In Figs. 4a and 4b, the variation of AM $m_{3,3}$ and RD $N_{3,3}$ corresponds to the pitch motion of the floating dock are plotted as a function of wavenumber $\hat{K}$ and for various values of $\hat{a}$.

Figure 4a shows that $m_{3,3}$ initially decreases as $\hat{K}$ increases and attains minimum. Hereafter, $m_{3,3}$ increases with an increase in $\hat{K}$. Further, it is observed that the AM $m_{3,3}$ increases with an increase in $\hat{a}$. Figure 4b shows that $N_{3,3}$ decreases as $\hat{K}$ increases. Moreover, the RD coefficient increases with an increase in $\hat{a}$.

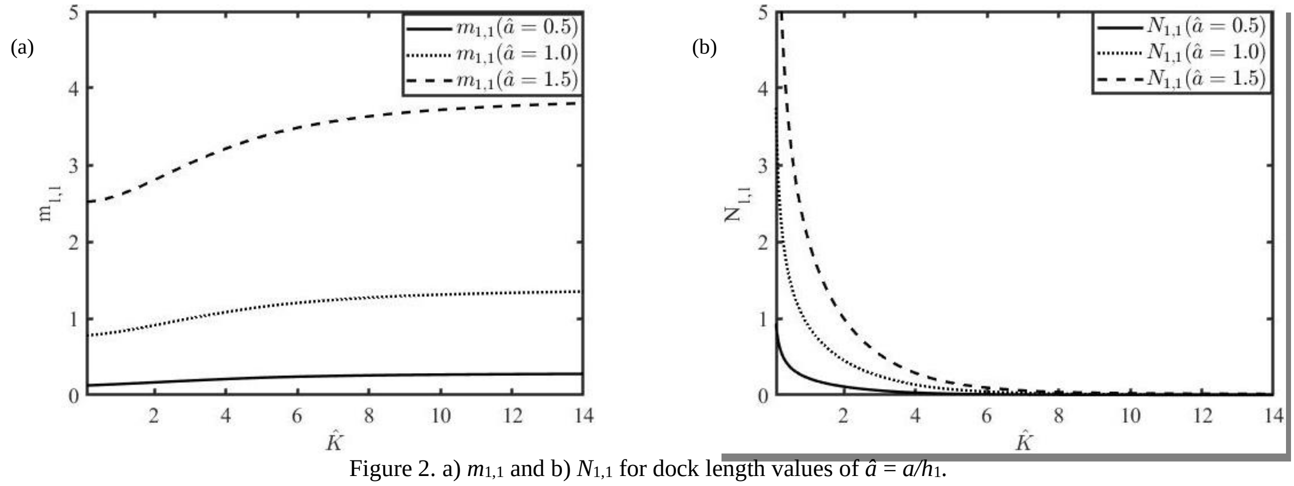

Figure 2. a) $m_{1,1}$ and b) $N_{1,1}$ for dock length values of $\hat{a} = a/h_1$.

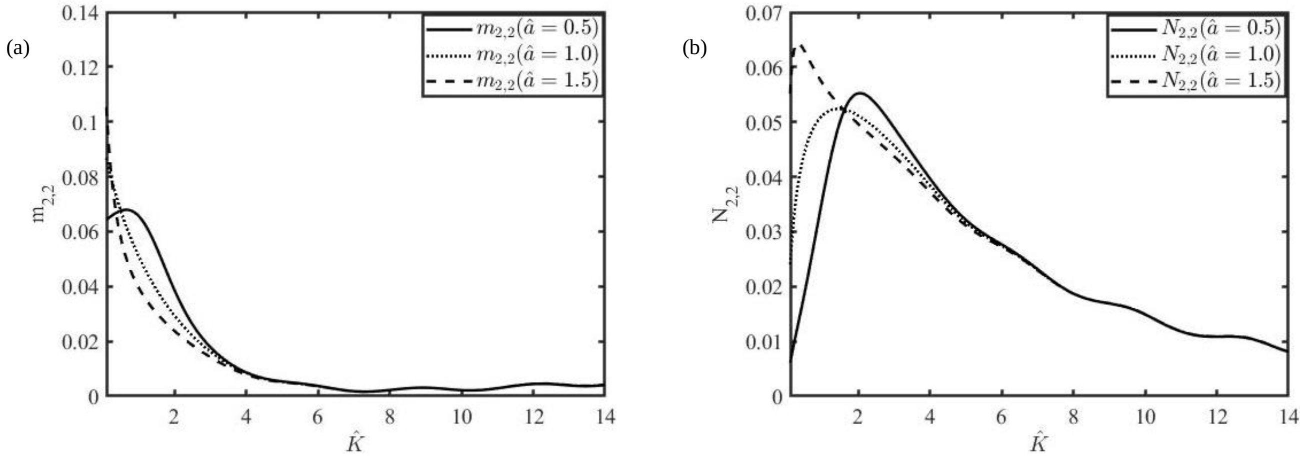

Figure 3. a) $m_{2,2}$ and b) $N_{2,2}$ for dock length values of $\hat{a}$.

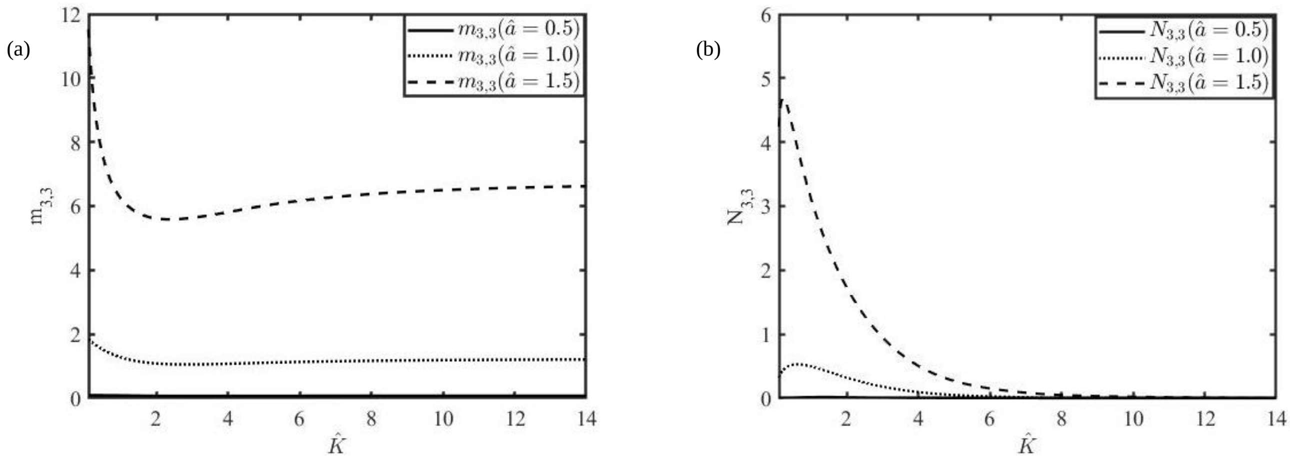

Figure 4. a) $m_{3,3}$ and b) $N_{3,3}$ for dock length values of $\hat{a}$.

CONCLUSIONS

In the present study, the motions of a freely floating thick rigid dock over the asymmetric trenches are analysed. To solve the associate BVP, the BEM method is used. Various physical parameters such as the AM and RD associated with the heave, surge, and pitch motions of the freely floating rigid structures are analysed for different values of dock length. It is observed that AM corresponds to the heave motion of the floating dock increase, and the related RD coefficient decreases with an increase in wavenumber. Further, the AM and RD coefficient increase for higher values of dock length. Further, it is seen that in the intermediate and shortwave regime, the AM and RD coefficient correspond to the surge motion of the floating dock and decrease with an increase in wavenumber. Moreover, the added mass corresponds to the pitch motion of the floating dock and initially decreases with increase in wavenumber and attains minimum. Hereafter, the added mass increases with an increase in wavenumber. A reverse pattern is noticed for the RD coefficient of the pitch motion of the dock. Moreover, the AM and RD coefficient correspond to the pitch motion and increase with an increase in dock length.

ACKNOWLEDGMENTS

KT and SK acknowledges the DST Project: DST/INSPIRE/04/2017/002460 to pursue this work. Further, SK acknowledges RIG project: BITS/GAU/RIG/2019/H0631 and Additional Competitive Research Grant: BITS/GAU/ACRG/2019/H0631.

REFERENCES

1. Lee, J.F. (1995), *On the heave radiation of a rectangular structure*, Ocean Eng. 22(1): 19-34. doi: 10.1016/0029-8018(93)E0009-H
2. Hsu, H.H., Wu, Y.C. (1997), *The hydrodynamic coefficients for an oscillating rectangular structure on a free surface with sidewall*, Ocean Eng. 24(2): 177-199. doi: 10.1016/0029-8018(96)00009-1
3. Williams, A.N., Lee, H.S., Huang, Z. (2000), *Floating pontoon breakwaters*, Ocean Eng. 27(3): 221-240. doi.org/10.1016/S0029-8018(98)00056-0
4. Zheng, Y.H., You, Y.G., Shen, Y.M. (2004), *On the radiation and diffraction of water waves by a rectangular buoy*, Ocean Eng. 31(8-9): 1063-1082. doi: 10.1016/j.oceaneng.2003.10.012
5. Zheng, Y.H., Shen, Y.M., You, Y.G., et al. (2004), *On the radiation and diffraction of water waves by a rectangular structure with a sidewall*. Ocean Engineering, 31(17-18): 2087-2104. doi: 10.1016/j.oceaneng.2004.06.002
6. Shen, Y.M., Zheng, Y.H., You, Y.G (2005), *On the radiation and diffraction of linear water waves by a rectangular structure over a sill. Part I. Infinite domain of finite water depth*. Ocean Eng. 32(8-9): 1073-1097. doi: 10.1016/j.oceaneng.2004.07.011
7. Zheng, Y.H., Shen, Y.M., You, Y.G., et al. (2006), *Wave radiation by a floating rectangular structure in oblique seas*, Ocean Eng. 33(1): 59-81. doi: 10.1016/j.oceaneng.2005.04.005
8. Zhou, H.W., Wu, G.X., Zhang, H.S. (2013), *Wave radiation and diffraction by a two-dimensional floating rectangular body with an opening in its bottom*, J Eng. Math. 83(1): 1-22. doi: 10.1007/s10665-012-9609-2
9. Zheng, S., Zhang, Y. (2016), *Wave diffraction and radiation by multiple rectangular floaters*, J Hydraul. Res. 54(1): 102-115. doi: 10.1080/00221686.2015.1090492
10. Katsikadelis, J.T., The Boundary Element Method for Engineers and Scientists: Theory and Applications, 2nd Ed., Academic Press, 2016.
11. Koley, S., Trivedi, K. (2020), *Mathematical modeling of oscillating water column wave energy converter devices over the undulated sea bed*, Eng. Anal. Bound. Elem. 117: 26-40. doi: 10.1016/j.enganabound.2020.03.017